Supplementary Information

Enhanced Minority Carrier Lifetimes in GaAs/AlGaAs Core-shell Nanowires Through Shell Growth Optimization

N. Jiang, Q. Gao*, P. Parkinson[¶], J. Wong-Leung*[§], S. Mokkapati*, S. Breuer*, H. H. Tan*, C. L. Zheng[†], J. Etheridge[†‡], and C. Jagadish**

* Department of Electronic Materials Engineering, Research School of Physics and Engineering, The Australian National University, Canberra, ACT 0200, Australia

¶ Clarendon Laboratory, Department of Physics, University of Oxford, Parks Road, Oxford, OX1 3 PU, United Kingdom

§ Centre for Advanced Microscopy, The Australian National University, Canberra, ACT 0200, Australia

† Monash Centre for Electron Microscopy, Monash University, Victoria 3800, Australia

‡ Department of Materials Engineering, Monash University, Victoria 3800, Australia

Corresponding Author

* Email: nxj109@physics.anu.edu.au

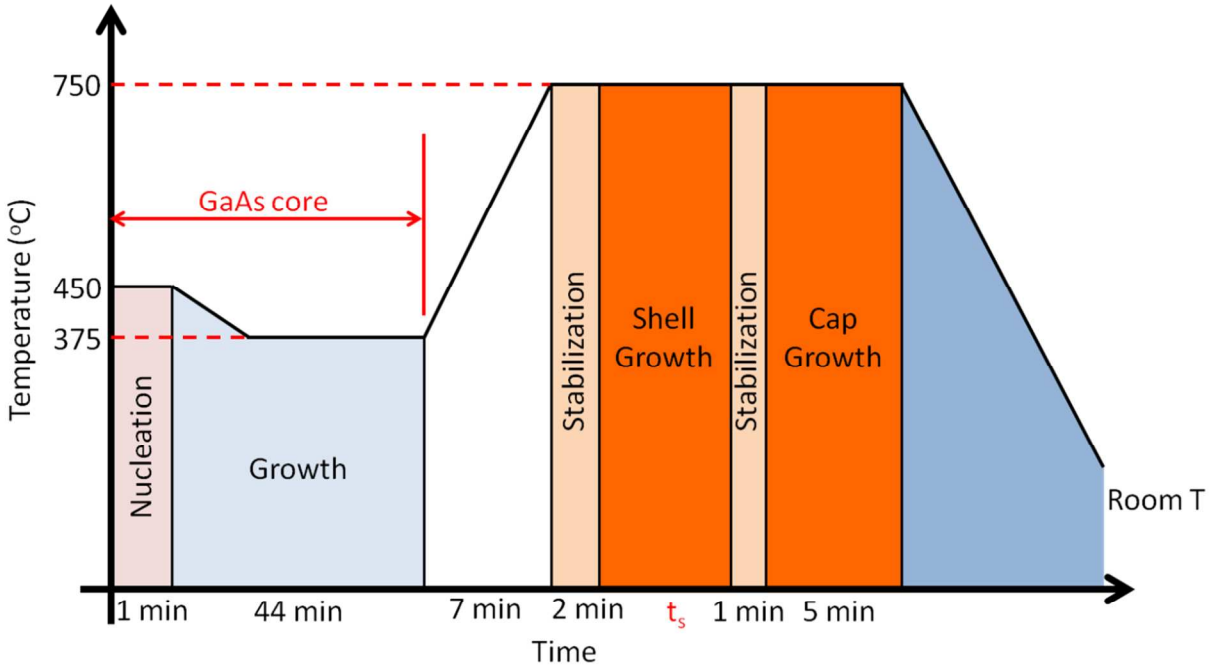

Figure S1.A schematic showing the growth of GaAs/AlGaAs core-shell nanowire growth. After GaAs core growth, the temperature of the reactor is increased to 750 ^{o}C with a 2 min stabilization period before growth of the AlGaAs shell. After shell growth, 1 min was allocated for stabilizing the gas flows for the GaAs cap growth. Interdiffusion occurred once the GaAs-core/AlGaAs-shell interface was formed and during the time for the shell and cap growth

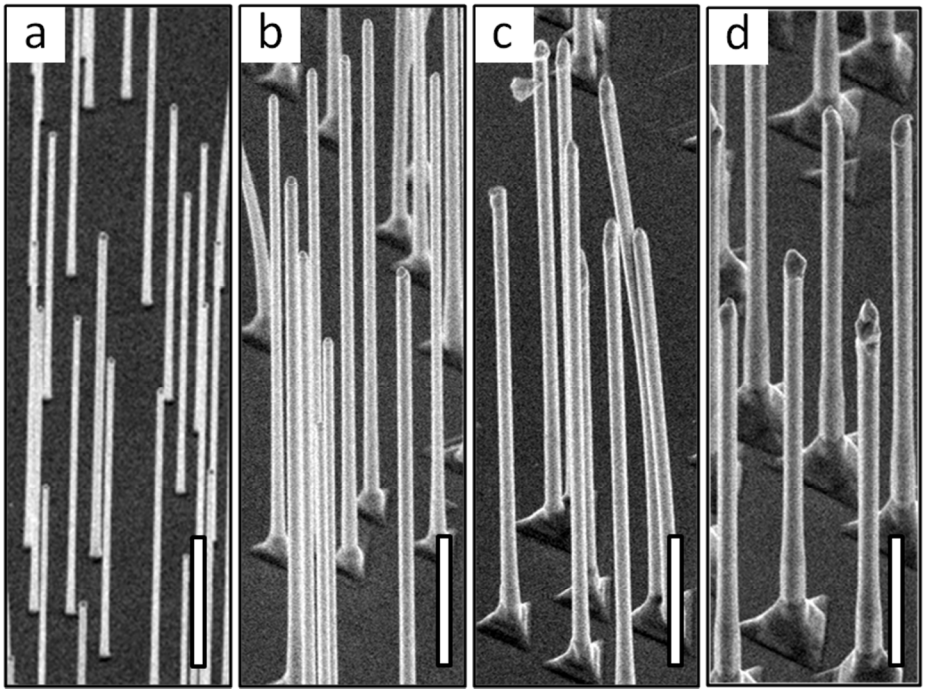

Bare GaAs t_s = 1.5 min t_s = 3 min t_s = 8 min

Figure S2. FESEM images of bare-GaAs nanowires and GaAs/AlGaAs core-shell nanowires with different shell growth times, t_s. All nanowires grew vertically on GaAs (111) B substrate with smooth and parallel sidewall facets. Scale bars are 1 μm.

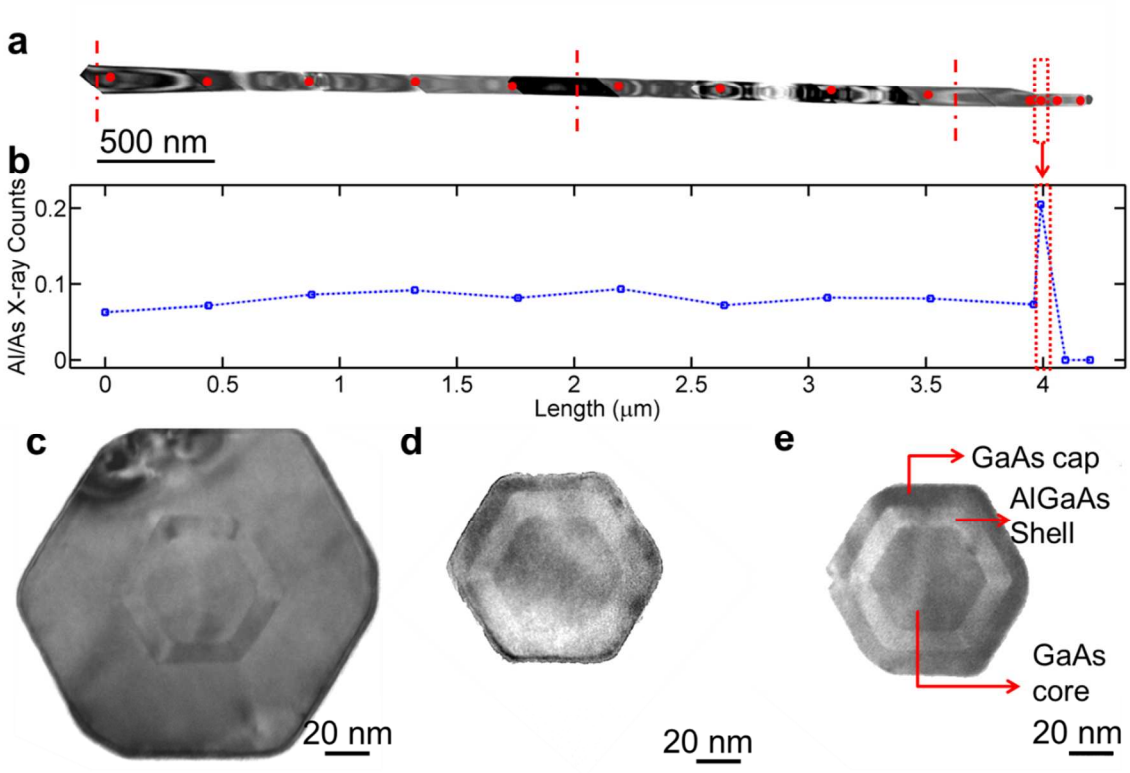

Figure S3. (a) A conventional bright field TEM image of a core-shell nanowire with 1.5 min shell growth time. The core-shell nanowire is stacking fault free along the length of the nanowire. Red dots on the wire indicate the positions where EDX measurements were taken. The red dotted box indicates unintentional AlGaAs axial growth during the shell growth. (b) EDX counts ratio of Al/As along the nanowire. Note that The Al/As X-ray counts ratio recorded in this geometry can only identify whether there is any change in the Al distribution along the wire axis but cannot distinguish the absolute Al mole fraction in the AlGaAs shell. The EDX results show that the Al concentration is approximately uniform along the nanowire and increases at the unintentionally grown AlGaAs axial segment followed by a drop to 0 at the unintentionally grown axial GaAs segment during the GaAs cap growth (c-e) Cross-sectional bright field images of core-shell nanowires at positions marked by vertical dashed line in (a). The facets are along the {110} planes. The AlGaAs shell thicknesses (L_b) for nanowires with different shell growth

time (normal growth rate, $III_o = 1.5 \times 10^{-5}$ mol/min) are measured from a few cross-sections and results are shown in Figure S4.

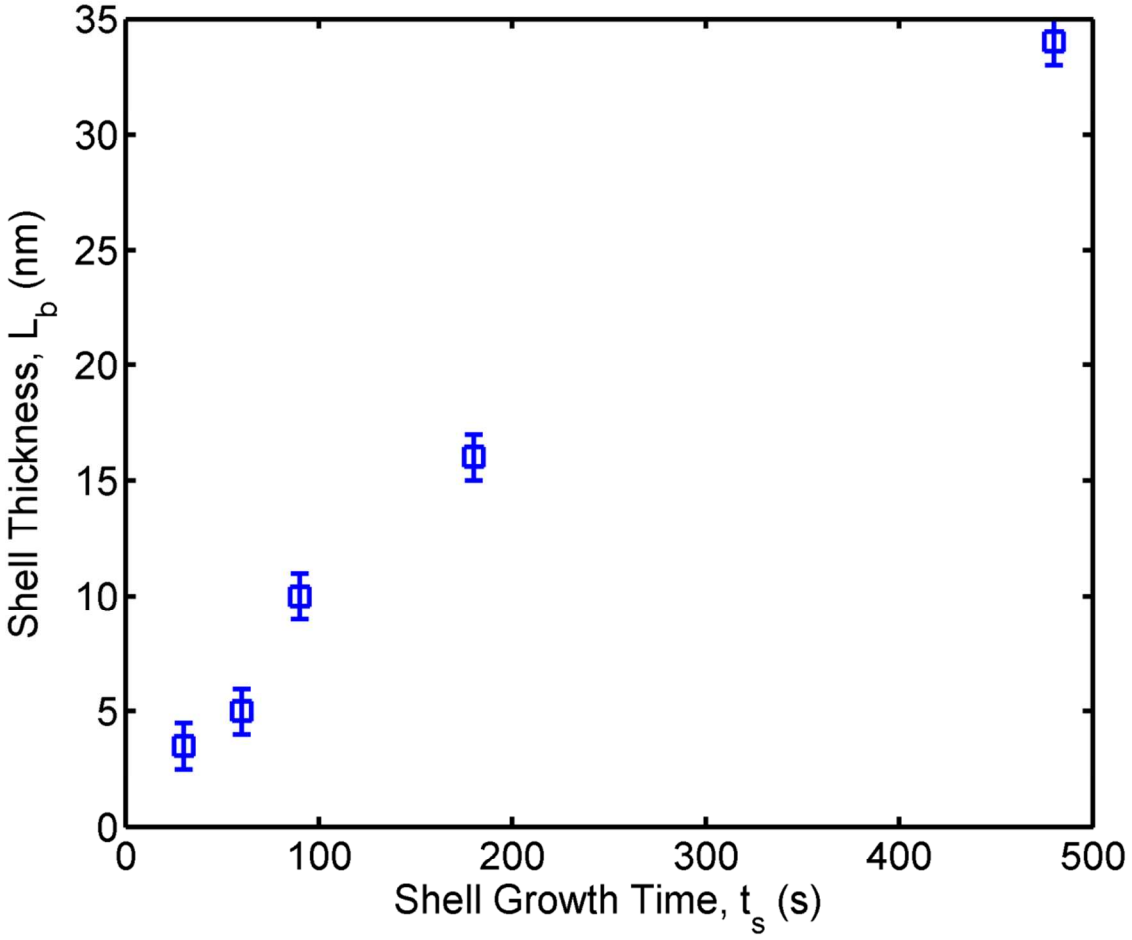

Figure S4. AlGaAs shell thickness (L_b) versus shell growth time (t_s) for samples with normal shell growth rate (III_o = 1.5 × 10^{-5} mol/min). L_b is measured from the cross-sectional TEM images.

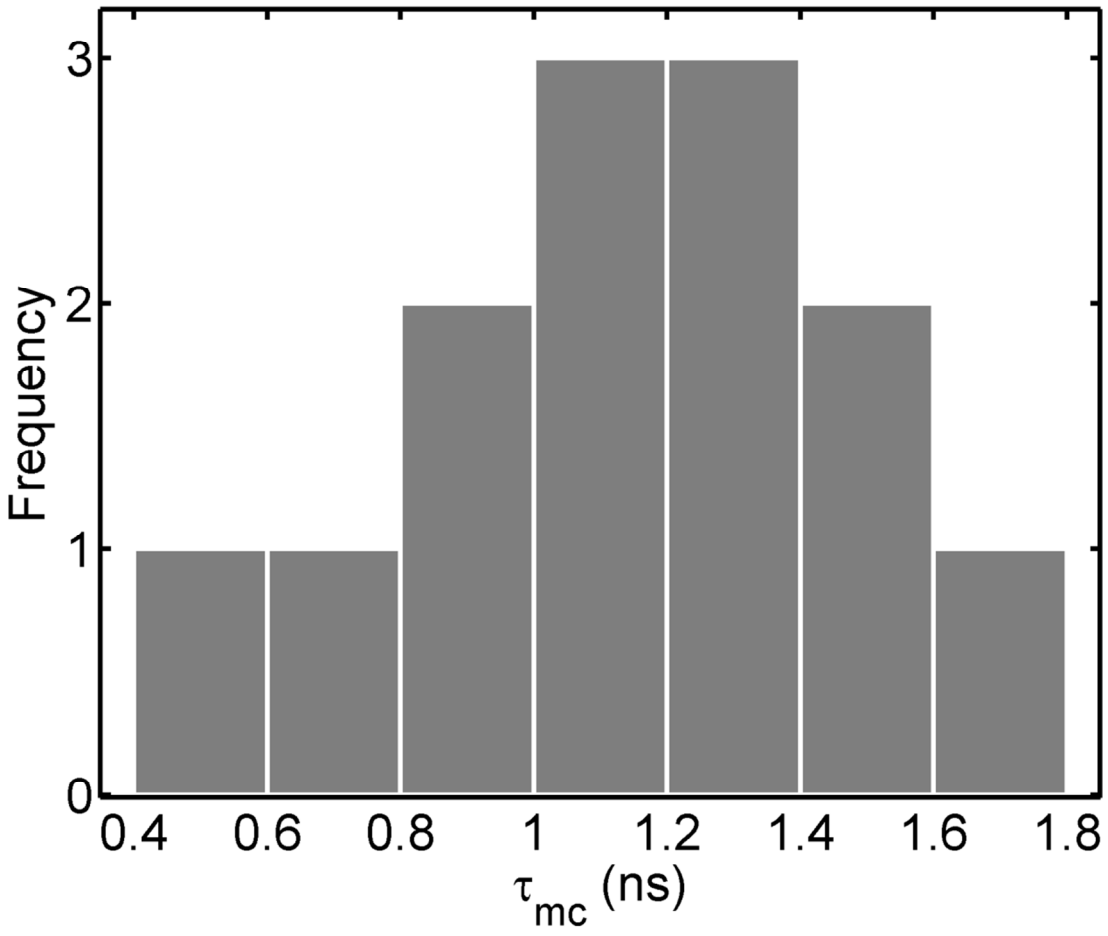

Figure S5. Statistics of measured lifetimes (τ_{mc}) of the sample with 3 min shell growth (shell thickness of 16 nm). 13 nanowires were randomly picked from two growths with identical growth parameters which were used to test the reproducibility.

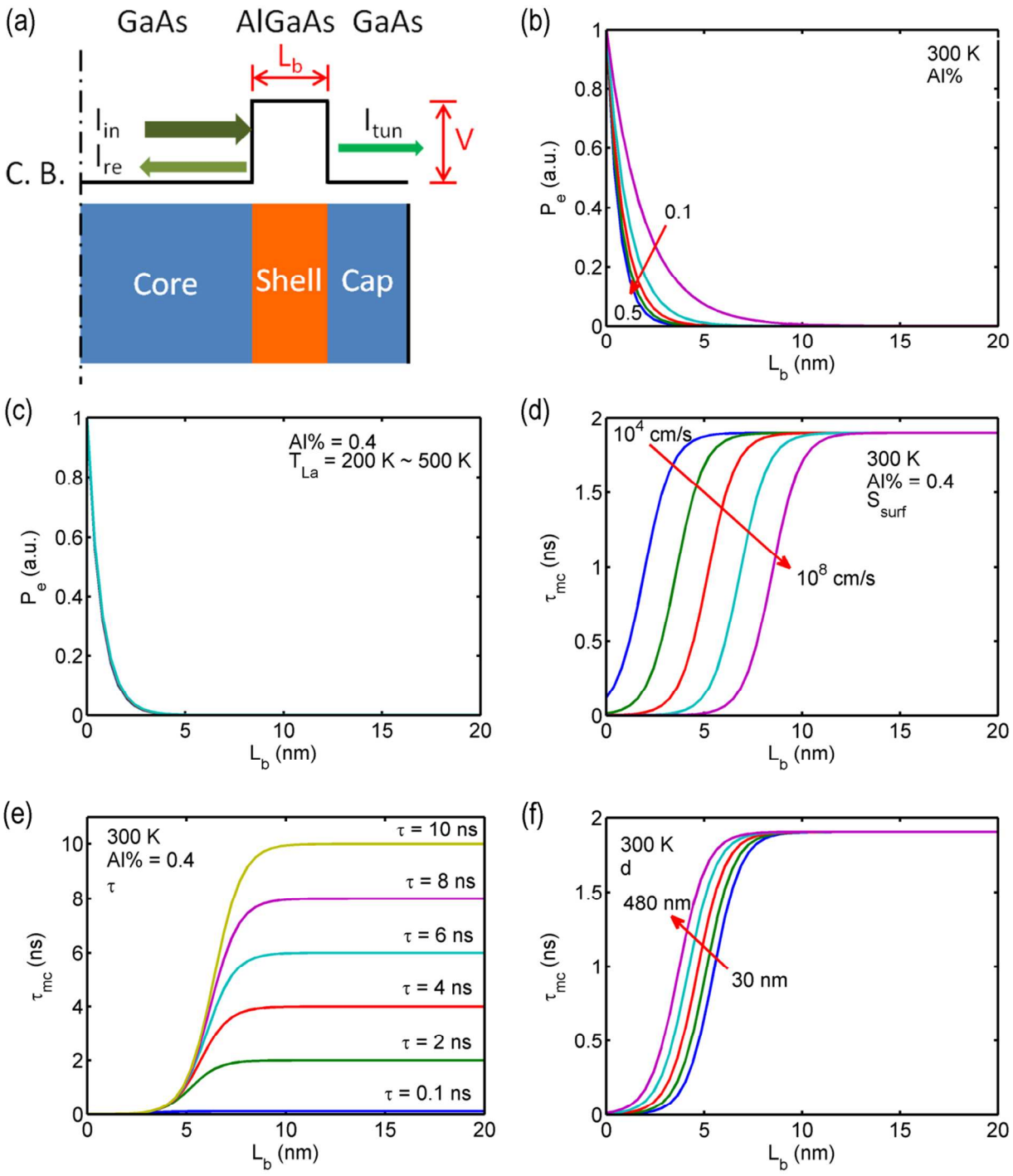

Simulation:

Figure S6. (a) Conduction band (C. B.) diagram of a GaAs/AlGaAs/GaAs core-shell-cap nanowire. No quantum confinement is taken into account since the radius of the GaAs core nanowires is larger than Bohr radius for an exciton in GaAs. I_{in} represents the incident current

density, I_{re} the reflected current density and I_{tun} the tunnelling current density. V represents the conduction band offsets and L_b the barrier thickness. (b-c) The effect of lattice temperature (T_{La}) and Al concentration of the AlGaAs shell on the tunnelling probability of electrons in the core (P_e) as a function of L_b, respectively. (d-f) The effect of surface recombination velocity (S_{surf}), saturated minority carrier lifetime in the core (τ) and the diameter of the core (d) on minority carrier lifetime (τ_{mc}) as a function of L_b, respectively. τ is considered as the minority carrier lifetime in the core when the effect of P_e on τ_{mc} vanishes. The effect of non-radiative recombination velocity at the core-shell interface (S_{int}) is incorporated in τ.

Considering a rectangular barrier provided by the AlGaAs shell, the tunnelling probability of electrons in the core, P_e is[1]

$$P_e = \frac{I_{in} - I_{re}}{I_{in}} = \frac{I_{tun}}{I_{in}} \propto \frac{16k^2\kappa^2}{(k^2+\kappa^2)^2}\exp(-2\kappa L_b),$$

where $k = \left(\frac{2m_oE}{\hbar^2}\right)^{\frac{1}{2}}$

and $\kappa = \left(\frac{2m_o(V-E)}{\hbar^2}\right)^{1/2}$

$\hbar$ is the reduced Planck constant, m_o the effective mass. E represents the energy of the carriers. This energy is primarily thermal energy in this study, given by $E \approx k_bT_{La}$ (where k_b is the Boltzmann constant). T_{La} can be obtained by fitting the high energy tail of the PL spectrum. E will increase P_e by thermally activated the carriers in GaAs core to AlGaAs shell. For GaAs, m_o = 0.063m. V is a function of Al concentration in AlGaAs, V = 0.77 × Al%. Figure S6(b) shows the effect of Al% on P_e. While 50% of Al is used in vapour phase for the AlGaAs shell growth, the incorporated Al was estimated to be about 40%,[2] which makes V = 308 meV. Since V is much higher than E (~ 26 meV at 300 K), the contribution of thermal activation to P_e is negligible, as shown in Figure S6(c) that P_e does not change much with T_{La} in the range of 300 ~

500 K. With an effective mass of $0.51m_o$ for the holes confined in valence band, the tunnelling probability of heavy holes in the core is much lower than P_e; thus only P_e is considered in this simulation.

For a nanowire,[3]

$$\frac{1}{\tau_{mc}} = \frac{1}{\tau_r} + \frac{1}{\tau_{b,non}} + \frac{4S_{surf}}{d}$$

where τ_r is the radiative recombination lifetime, $\tau_{b,non}$ is the non-radiative recombination lifetime of bulk material, S_{surf} is surface recombination velocity of GaAs which is about 10^6 cm/s[4,5] and d is the diameter of nanowire. According to this equation, τ_{mc} strongly depends on the third term which includes both the diameter and S_{surf} . In order to study the effect of S_{surf}, the diameter of GaAs core nanowires was fixed in this study; in this way, S_{surf} is the only independent variable. If tunnelling is taken into account,

$$\frac{1}{\tau_{mc}} = \frac{1}{\tau_r} + \frac{1}{\tau_{b,non}} + \frac{4S_{int}}{d} + P_e\frac{4S_{surf}}{(d + 2L_b)} = \frac{1}{\tau} + P_e\frac{4S_{surf}}{(d + 2L_b)}$$

$$\frac{1}{\tau} = \frac{1}{\tau_r} + \frac{1}{\tau_{b,non}} + \frac{4S_{int}}{d}$$

where τ represents the τ_{mc} when L_b is thick enough to eliminate tunnelling effect. While S_{int} is dominated by the interdiffusion in this study, the longest measured τ_{mc} is used to represent τ where the effect of interdiffusion on τ_{mc} is excluded. For AlGaAs passivated GaAs nanowires, S_{int} is typical in a range of 10^3 cm/s or even lower[6,7] which is 3 orders of magnitudes smaller than S_{surf}. This will magnify the effect of P_e on τ_{mc} and make τ_{mc} extremely sensitive to P_e, (Figure S6(d)), which explains the difference in L_b where τ_{mc} saturated, $L_{b,s}$ and where P_e falls to 0 in Figure 1(c). The effect of τ on τ_{mc} is also displayed in Figure S6(e). τ will not have a significant impact on $L_{b,s}$ once it is in ns range. By comparing Figure S6(d), (e) and (f), it is found that S_{surf} is the dominant parameter which determines $L_{b,s}$.

References

(1) Miller, D. A. B. *Quantum Mechanics for Scientists and Engineers*; Cambridge University Press: United States of America, 2008.

(2) Mokkapati, S.; Saxena, D.; Jiang, N.; Parkinson, P.; Wong-Leung, J.; Gao, Q.; Tan, H. H.; Jagadish, C. *Nano Lett.* **2012**, *12*, 6428.

(3) Breuer, S.; Pfuller, C.; Flissikowski, T.; Brandt, O.; Grahn, H. T.; Geelhaar, L.; Riechert, H. *Nano Lett.* **2011**, *11*, 1276.

(4) Lloyd-Hughes, J.; Merchant, S. K. E.; Fu, L.; Tan, H. H.; Jagadish, C.; Castro-Camus, E.; Johnston, M. B. *Appl. Phys. Lett.* **2006**, *89*, 232102.

(5) Demichel, O.; Heiss, M.; Bleuse, J.; Mariette, H.; Fontcuberta i Morral, A. *Appl. Phys. Lett.* **2010**, *97*, 201907.

(6) Prechtel, L.; Padilla, M.; Erhard, N.; Karl, H.; Abstreiter, G.; Fontcuberta i Morral, A.; Holleitner, A. W. *Nano Lett.* **2012**, *12*, 2337.

(7) Jiang, N.; Parkinson, P.; Gao, Q.; Breuer, S.; Tan, H. H.; Wong-Leung, J.; Jagadish, C. *Appl. Phys. Lett.* **2012**, *101*, 023111.